



## Molecular Crystals and Liquid Crystals

Publication details, including instructions for authors and subscription information:

<http://www.tandfonline.com/loi/gmcl20>

### DNA Condensation into Inverted Hexagonal Phase in Aqueous Dispersion of Poly(Ethylene)-Functionalized Dioleoylphosphatidylethanolamine and Metal Cations

M. Pisani<sup>a</sup>, V. Fino<sup>a</sup>, P. Bruni<sup>a</sup> & O. Francescangeli<sup>b</sup>

<sup>a</sup> Dipartimento di Scienze e Tecnologie Chimiche and CNISM, Università Politecnica delle Marche, Via Brecce Bianche, Ancona, Italy

<sup>b</sup> Dipartimento di Fisica e Ingegneria dei Materiali e del Territorio and CNISM, Università Politecnica delle Marche, Via Brecce Bianche, Ancona, Italy

Version of record first published: 18 Mar 2009

To cite this article: M. Pisani, V. Fino, P. Bruni & O. Francescangeli (2009): DNA Condensation into Inverted Hexagonal Phase in Aqueous Dispersion of Poly(Ethylene)-Functionalized Dioleoylphosphatidylethanolamine and Metal Cations, *Molecular Crystals and Liquid Crystals*, 500:1, 132-143

To link to this article: <http://dx.doi.org/10.1080/15421400802714080>

PLEASE SCROLL DOWN FOR ARTICLE

Full terms and conditions of use: <http://www.tandfonline.com/page/terms-and-conditions>

This article may be used for research, teaching, and private study purposes. Any substantial or systematic reproduction, redistribution, reselling, loan, sub-licensing, systematic supply, or distribution in any form to anyone is expressly forbidden.

The publisher does not give any warranty express or implied or make any representation that the contents will be complete or accurate or up to date. The accuracy of any instructions, formulae, and drug doses should be independently verified with primary sources. The publisher shall not be liable for any loss, actions, claims, proceedings, demand, or costs or damages whatsoever or howsoever caused arising directly or indirectly in connection with or arising out of the use of this material.

## DNA Condensation into Inverted Hexagonal Phase in Aqueous Dispersion of Poly(Ethylene)-Functionalized Dioleoylphosphatidylethanolamine and Metal Cations

M. Pisani<sup>1</sup>, V. Fino<sup>1</sup>, P. Bruni<sup>1</sup>, and O. Francescangeli<sup>2</sup>

<sup>1</sup>Dipartimento di Scienze e Tecnologie Chimiche and CNISM, Università Politecnica delle Marche, Via Brecce Bianche, Ancona, Italy

<sup>2</sup>Dipartimento di Fisica e Ingegneria dei Materiali e del Territorio and CNISM, Università Politecnica delle Marche, Via Brecce Bianche, Ancona, Italy

*We report the x-ray diffraction study of the structure and phase behavior of mixtures of dioleoylphosphatidylethanolamine (DOPE) and poly(ethyleneglycol)-functionalized DOPE (DOPE:PEG(350)) in aqueous dispersions of DNA and bivalent metal cations. Characterization of the phase behaviour of DOPE/DOPE:PEG(350) mixtures in presence of metal cations without DNA is also performed: over a definite amount of the PEG-lipid component, a phase transition from the inverted hexagonal phase  $H_{II}$  to the bicontinuous inverted cubic phase, with space group  $Pn3m$  is induced. Moreover, it is shown that at low concentration of PEG-lipid component, the inverted hexagonal phase ( $H_{II}^*$ ) is found on adding DNA to the aqueous dispersions of DOPE/DOPE:PEG and metal cations. This structure consists of cylindrical DNA strands coated by neutral lipid monolayers and arranged on a two-dimensional hexagonal lattice. The results here shown represent the first experimental evidence of a self-assembled formation of an inverted hexagonal complex structure in aqueous dispersions of DNA, metal cations and liposomes made of mixtures of pure and pegylated lipids. The surface functionalization with the PEG-lipid and the evidence of the formation of the complexes are important results in the perspective of the development of appropriate vectors for drug delivery and gene transfection.*

**Keywords:** complexes; DOPE; DNA; PEG; x-ray diffraction

## INTRODUCTION

Gene therapy is a promising technique for correcting the defective genes responsible for disease development. The goal is to achieve the

Address correspondence to M. Pisani, Dipartimento di Scienze e Tecnologie Chimiche, Università Politecnica delle Marche, Via Brecce Bianche, Ancona I-60131, Italy. E-mail: m.pisani@univpm.it

transfer of extracellular genetic material into somatic cells and thereby provide therapeutic effects. The development of gene therapy strictly depends on the availability of safe and efficient gene delivery vectors. These vectors may be either viral or nonviral and nowadays great progress is being made in all areas of vector technology, owing to an improved biophysical characterisation of the whole process and an increasing insight into the mechanisms of delivery routes. Cationic liposomes are the most studied among synthetic vectors because of their low levels of immunogenicity, toxicity and oncogenicity, and the possibility of a wide range of applications joined with their simple production. However, three major problems are still dealing with the use of cationic liposomes: (i) lack of efficacy in *in vivo* transfection, (ii) some level of cytotoxicity and (iii) weak stability of their complexes with plasmid DNA (lipoplexes) in serum. Referring to transfection efficiency, the search for better vectors is therefore of strategic importance [1] and most studies are presently concerned with new synthetic liposomes.

Over the last few years our interest in the field of non viral vectors for DNA delivery has been focused on neutral (zwitterionic) liposomes, due in particular to the intrinsic absence of cytotoxicity. Unfortunately, the lack of a positive net charge in such compounds makes the association with DNA rather weak. More stable complexes are obtained when neutral liposomes (L) and DNA are mixed in water solutions of metal cations ( $M^{2+}$ ), namely  $Ca^{2+}$ ,  $Mg^{2+}$ , and  $Mn^{2+}$ : in such conditions stable ternary complexes L-DNA- $M^{2+}$  are easily formed [2] in a self assembled manner. X-ray diffraction (XRD) studies of these systems have shown different structures including lamellar phase, in which the hydrated DNA helices are sandwiched between the liposome bilayers [2,3], and inverted hexagonal phase, where DNA strands are hosted inside the cavity of the hexagonal lattice of dioleylphosphatidylethanolamine (DOPE) [4]. Recently it has been found that the incorporation of synthetic lipids conjugated with poly(ethyleneglycol) (PEG lipids) into liposomes makes these systems to act as effective *in vivo* drug delivery agents [5]. The presence of PEG-lipids in the vector creates a steric barrier that inhibits opsonization and prevents the interaction of lipoplexes (lipid-DNA or amphiphilic-DNA complexes) with serum proteins and macrophages, therefore prolonging their circulation lifetime in blood [6,7]. Due to the higher circulation lifetime of PEG- liposomes and the leak of the microcirculation in solid tumors, these systems behave as efficient anticancer drug vectors in the therapy of tumors [8–10]. In addition, the use of DOPE, which promotes fusion and destabilizes target endosomal membranes, strongly favors the transfection efficiency [11].

Based on such considerations, it is of both fundamental and applicative interest to investigate the structure and phase behavior of lipid/PEG-lipid mixtures. The structure of the PEG-lipid mixtures and the formation of a steric barrier in the PEG-liposomes depend on the ability of the lipids to self-assemble into stable bilayers: the effects of the PEG molecular weight and of the different PEG-lipid concentrations on the bilayer structure are still far to be fully understood [12].

In this work we report the XRD study of the structure and phase behavior of DOPE/DOPE:PEG(350) mixtures with different amount of the PEG-lipid fraction, in aqueous solution of bivalent metal cations ( $M^{2+}$ ) with and without DNA. At low concentrations of the PEG-lipid component we observe the self-assembled condensation of DNA into the inverted hexagonal structure  $H_{II}^c$  in which the DNA strands fill the water space inside the cylindrical cavities of the DOPE/DOPE:PEG(350) hexagonal lattice. The release of the counterion entropy upon the neutralization of the DNA-phosphate groups promoted by the metal cations drives the self assembled formation of the ternary DOPE/DOPE:PEG(350)-DNA- $M^{2+}$  complexes and stabilizes their structure by binding the DOPE/DOPE:PEG(350) polar headgroup to the phosphate groups of DNA. This result represents the first experimental evidence of a self-assembled formation of an inverted hexagonal complex structure in aqueous dispersions of DNA, metal cations and liposomes made of mixtures of pure and pegylated (PEG) lipids. The fact that the hexagonal structures are more fusogenic than the corresponding lamellar ones and that the coating of the vector due to PEG makes the resulting object more stable on serum, leads our synthetic systems to be particularly promising for gene delivery applications.

## EXPERIMENTAL METHODS

### Materials and Sample Preparation

1,2-Dioleoyl-*sn*-Glycero-3-Phosphatidylethanolamine (DOPE), 1,2-dioleoyl-*sn*-glycero-3-phosphoethanolamine-N-[methoxy(polyethylene glycol)-350] (DOPE:PEG(350)) were purchased from Avanti Polar Lipids inc (Alabaster, USA), DNA from calf thymus and anhydrous  $MnCl_2$  and  $CaCl_2$  were purchased from Sigma-Aldrich co. (Stenheim, Germany). Lipid mixtures were suspended in 20 mM aqueous solutions of (N-[2-hydroxyethyl]piperazine-N'-[ethanesulphonic acid]) (HEPES) obtained from Sigma-Aldrich co. The DNA aqueous solution (13 mg/ml) was sonicated in order to induce a DNA fragmentation whose length distribution, detected by gel electrophoresis, varied between

500 and 2000 bp. All chemicals were used without further purification and preparation of sample was performed using milliQ water. DOPE (78 mM) and DOPE:PEG(350) lipid at variable amount (from 3 to 25% wt) were codissolved in chloroform solution and the solvent was removed under vacuum with the Speedvac<sup>®</sup> apparatus and the residue hydrated in HEPES buffer (pH=7.4). The aqueous suspension of complexes were prepared mixing the DOPE–DOPE: PEG(350) lipids mixture with the solutions of metal chloride (585 mM) and DNA (39 mM) in HEPES buffer. The samples were finally incubated over one week at 4°C.

### X-ray Diffraction

XRD measurements were carried out at the high brilliance beamline ID02 of the European Synchrotron Radiation Facility (Grenoble, France). The energy of the incident beam was 12.5 keV ( $\lambda = 0.995 \text{ \AA}$ ), the beam size was  $100 \times 100 \mu\text{m}^2$ , and the sample-to-detector distance was 1.2 m. The 2D diffraction patterns were collected by a CCD detector. We investigated the small angle range from  $q_{\min} = 0.1 \text{ nm}^{-1}$  to  $q_{\max} = 4 \text{ nm}^{-1}$  with a resolution of  $5 \times 10^{-3} \text{ nm}^{-1}$  (FWHM). The sample was held in a 1 mm-sized glass capillary. To avoid radiation damage, each sample was exposed to radiation for mostly 3 sec/frame.

In order to calculate the electron density map of DOPE/DOPE:PEG(350) in the  $H_{II}$  phase, the integrated intensities of the diffraction peaks were determined by fitting the data with series of Lorentz functions using a nonlinear baseline. The Lorentz correction was performed by multiplying each integrated intensity by  $\sin\theta$  and the intensities were then calibrated by dividing by the multiplicity of the reflection [13,14]. The square root of the corrected peak was finally used to determine the modulus of the form factor  $F$  of each respective reflection. The electron density profile within the unit cell was calculated by Fourier synthesis, which for the  $p6$  space group of our hexagonal lattice reads [15]

$$\rho(x,y) = \frac{1}{A_c} \left[ F(00) + 2 \left\{ \sum_{h=1}^{\infty} F_{h,0} \cos(2\pi hx) + \sum_{k=1}^{\infty} F_{0,k} \cos(2\pi ky) \right\} + 2 \left\{ \sum_{h=1}^{\infty} \sum_{k=1}^{\infty} F_{h,k} \cos(2\pi(hx + ky)) + \sum_{h=1}^{\infty} \sum_{k=1}^{\infty} F_{-h,k} \cos(2\pi(hx - ky)) \right\} \right]$$

where  $x$  and  $y$  are the coordinates in the unit cell,  $A_c$  is the area of the unit cell and  $F_{h,k}$  is the form factor of the  $(hk)$  reflection (a real number, either positive or negative, for centrosymmetric structures).

The best phasing choice (+ - - + + + +) was obtained following the phasing criteria developed by Harper *et al.* [13].

## RESULTS AND DISCUSSION

We started studying the effect of the concentration ( $c$ ) on the mesomorphic behavior of the phospholipid in water of the DOPE: PEG component in the DOPE/DOPE:PEG(350) mixture [16]: representative small angle XRD patterns are shown in Figure 1. At low concentrations of DOPE:PEG(350) ( $c < \cong 9\%$ ) the system exhibits the inverted hexagonal phase  $H_{II}$ , as indicated by the set of Bragg peaks that can be indexed on a 2D hexagonal lattice according to  $q_{hk} = 4\pi(h^2 + hk + k^2)^{1/2}/\sqrt{3}a$ , being  $a$  the lattice constant,  $q_{hk}$  the measured peak position and  $h, k$  the Miller indices. In this phase the structure elements are infinitely long rigid rods, all identical and crystallographically equivalent, regularly packed in a 2D hexagonal lattice.

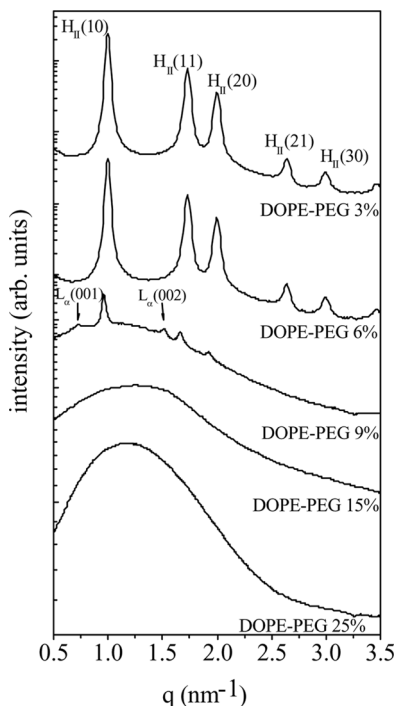


**FIGURE 1** Synchrotron SAXS patterns of aqueous dispersion of DOPE/DOPE:PEG(350) mixtures at different concentration of DOPE:PEG(350) component.

The cylinders are water filled and are regularly dispersed in the continuous matrix constituted by hydrocarbon chains, with the polar groups located at the water-hydrocarbon chain interface. The unit cell spacing  $a$  varies from 72.3 Å ( $c = 3\%$ ) to 75.2 Å ( $c = 9\%$ ), close to the value  $a = 74.4$  Å measured in pure DOPE [4]. At about  $c = 9\%$  of DOPE:PEG(350) the intensity of the peaks corresponding to  $H_{II}$  phase decrease and a new phase starts developing, associated with the growing of the two weak peaks denoted by L in Figure 1 and consistent with a lamellar phase  $L_\alpha$  having repeat distance  $d = 85.0$  Å. Such evolution of the XRD pattern indicates the higher energy cost of the elastic bending of the lipid layers in the hexagonal phase, as the PEG concentration increases. This leads to the decrease of the lipid spontaneous curvature that eventually favours the flat bilayer structure of the lamellar phase. Over  $c > 9\%$  the system moves to the micellar phase, as shown by the growth of the broad diffuse band in the small-angle region of the pattern.

In the next step we focused the study on the effects of metal cations ( $Mn^{2+}$ ,  $Ca^{2+}$ ) on the polymorphic behaviour of DOPE/DOPE:PEG(350) in aqueous solution. In these experiments the molar ratio of the binary (DOPE/DOPE:PEG(350))/ $M^{2+}$  system was fixed at 1:3. Figure 2 shows the relevant XRD spectra collected at different concentrations of the PEG-lipid component, in aqueous solution of  $Mn^{2+}$ . Between  $c = 3\%$  and  $c = 6\%$  we observe the hexagonal phase  $H_{II}$  with unit cell parameter similar to that found in the absence of metal cations. However, at higher concentration ( $9\% < c < 15\%$ ) a remarkable change of the pattern occurs, consistent with a transition from inverted hexagonal to bicontinuous inverted cubic phase [16]. In fact, the new set of Bragg peaks denoted by Q in the XRD pattern can be indexed according to cubic structure of the  $Pn3m$  space group (spacing ratio  $\sqrt{2} : \sqrt{3} : \sqrt{4} : \sqrt{6} : \sqrt{8} : \sqrt{9} : \sqrt{10}$ ) with lattice parameter  $a = 139.2$  Å. A similar behaviour was observed in aqueous dispersions of  $Ca^{2+}$ , with only a slight difference in the value of the lattice parameter  $a = 136.2$  Å. In this range of lipid-PEG concentration the cubic phase  $Pn3m$  coexists with the hexagonal phase whereas at  $c = 25\%$  only the  $Pn3m$  cubic phase is eventually observed.

These experimental findings clearly show that high concentrations of the PEG-lipid component destabilize the inverted hexagonal phase towards either a lamellar phase, in the absence of metal cations, either an inverted cubic phase, in the presence of metal cations. Therefore, to preserve the hexagonal structure (that should show better transfection activities in gene therapy applications) it is necessary to work with low concentration of the DOPE:PEG component. Following this guideline we have finally characterized the structure of

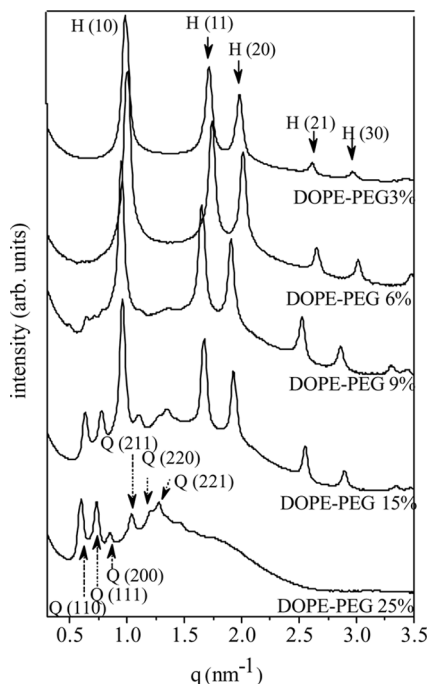


**FIGURE 2** Synchrotron SAXS patterns of aqueous dispersion of DOPE/DOPE:PEG(350) mixtures and  $\text{Mn}^{2+}$  as a function of different concentration of DOPE:PEG(350) component.

ternary DOPE/DOPE:PEG(350)-DNA- $\text{M}^{2+}$  mixtures ( $\text{M}^{2+} = \text{Ca}^{2+}$ ,  $\text{Mn}^{2+}$ ,  $\text{Mg}^{2+}$ ) in aqueous solution, fixing the DOPE:PEG(350) concentration at 3%. Figure 3 shows the diffraction pattern obtained in the presence of  $\text{Mn}^{2+}$  at a 2:1:6 molar ratio L-DNA- $\text{Mn}^{2+}$ . Two distinct sets of peak are clearly identified, labelled as  $H_{II}$  and  $H_{II}^c$ , which can be indexed on 2D hexagonal lattice with different unit cell,  $a = 74.2 \text{ \AA}$  and  $a_c = 68.2 \text{ \AA}$ , respectively. The first set of peaks corresponds to the  $H_{II}$  phase of DOPE/DOPE:PEG(350), whereas the second set is consistent with the 2D columnar inverted hexagonal structure, which we consider as the  $H_{II}^c$  phase of DOPE/DOPE:PEG(350)-DNA- $\text{Mn}^{2+}$  complex, where the DNA strands fill the water gap inside the cylinders of the structure of the phospholipid mixture. This hexagonal phase is similar to the ones observed for pure DOPE and DOPE/DOPE:PEG(350) mixture, with the difference that in the sample under consideration the water space inside the cylinders is filled by DNA. As previously found in the inverted hexagonal phase of the

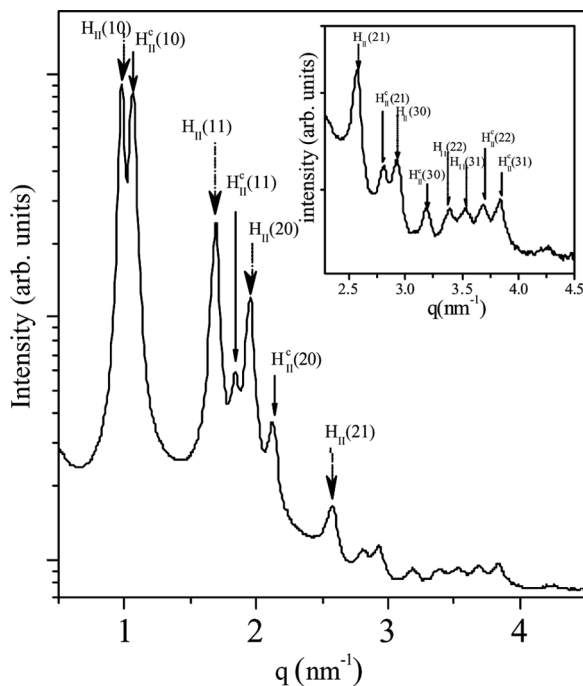


**FIGURE 3** Synchrotron SAXS patterns of the ternary DOPE/DOPE: PEG(350)-DNA-Mn<sup>2+</sup> mixtures in aqueous solution. The DOPE:PEG(350) concentration is 3%.

DOPE-DNA-Fe<sup>2+</sup> complex [4], also in this case the driving force for the lipid-DNA complexation is the release of counterion entropy upon neutralization of the DNA phosphate-groups operated by the metal cations in their role of bridge between the polar heads of the lipid and the negatively charged phosphate groups of DNA.

The formation of the complex structure  $H_{II}^c$  is also confirmed by the analysis of the electron density (ED) profiles along the [10] direction of the unit cell (see Ref. 4, Fig. 5), calculated from the XRD data as discussed in the experimental section and shown in Figures 4A and 4B for the uncomplexed ( $H_{II}$ ) and complexed ( $H_{II}^c$ ) structures, respectively. The ED profile also gives information on the internal structure of the unit cell. The two maxima of the ED profile correspond to the polar headgroups and the central minimum corresponds to the hydrocarbon chain region. Accordingly, the distance between the centers of the density maxima in Figure 4A gives the phosphate-to-phosphate group distance  $d_{pp} = 39 \text{ \AA}$ . However, this value underestimates the effective

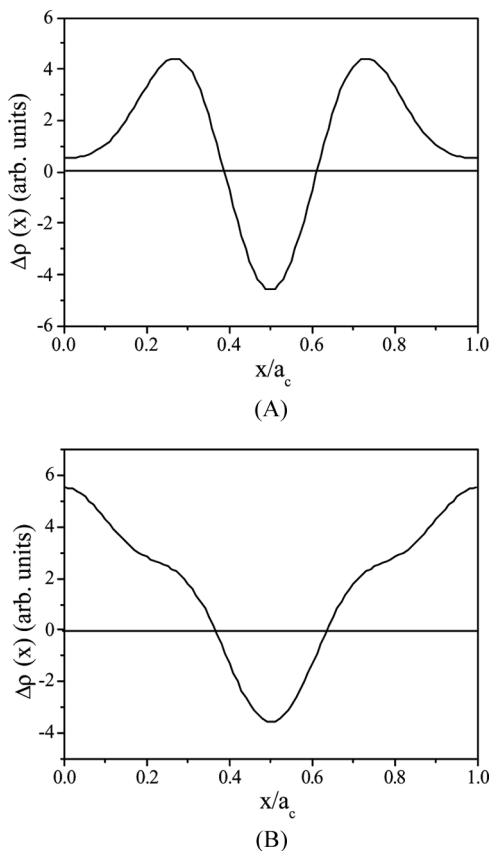


**FIGURE 4** (A) Electron density profile of DOPE/DOPE:PEG(350) hexagonal phase ( $H_{II}$ ) and (B) DOPE/DOPE:PEG(350)-DNA- $Mn^{2+}$  hexagonal phase ( $H_{II}^c$ ). Each minimum corresponds to the center of the water core of cylinders.

steric lipid bilayer thickness,  $d_L$ , because of the finite width of the headgroups [14,15]. A more reliable value of  $d_L$  is obtained by estimating the width of the headgroup,  $d_H$ , through the ED *Cylindrical Modelling* procedure described in Ref. [14]. For pure DOPE this model gives  $d_H = 11 \text{ \AA}$ , then the estimated lipid bilayer thickness is  $d_L = d_{PP} + d_H = 50 \text{ \AA}$ . Accordingly, the value of the diameter of water cylinders is here  $d_w = 2R_w = a - d_L = 24.2 \text{ \AA}$ , which is smaller than the diameter of water cylinders of pure DOPE ( $d_w = 30.2 \text{ \AA}$ ) [4].

Concerning the  $H_{II}^c$  phase, the ED profile of Figure 4B shows a strong increase of the electron density in the regions corresponding to the water cores, which is in agreement with the complex formation

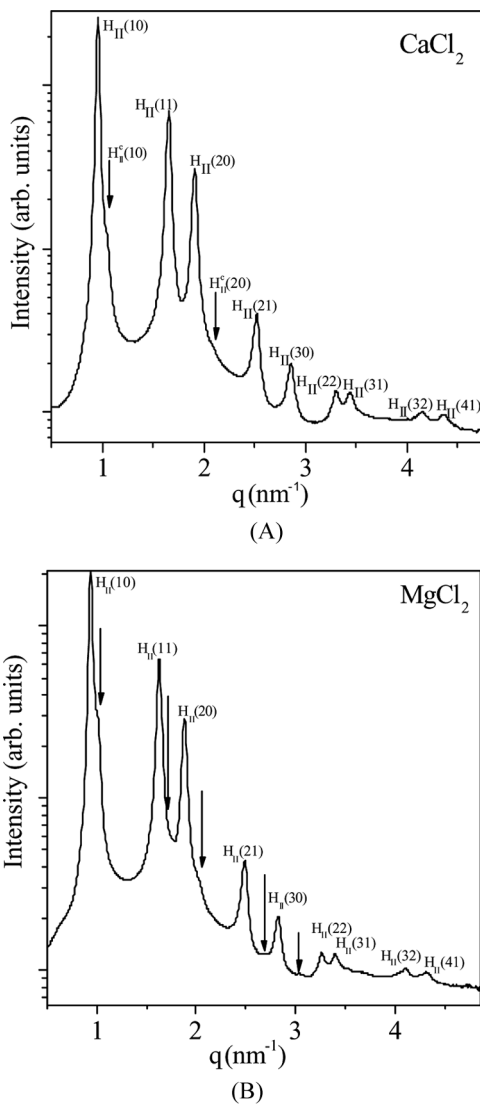


**FIGURE 5** Synchrotron SAXS patterns of the ternary DOPE/DOPE: PEG(350)-DNA- $M^{2+}$  mixtures. (A)  $M^{2+} = Ca^{2+}$ ; (B)  $M^{2+} = Mg^{2+}$ . The arrows indicate the complexed hexagonal phase ( $H_{II}^c$ ).

that leads the DNA strands to fill the cylindrical water gaps with consequent increment of the number of electrons per unit volume. The two shoulders observed at  $x/a_c = 0.26$  and  $x/a_c = 0.73$  correspond

to phosphorus and can be used to localize the centres of the polar head-groups. From the structural data, following the same procedure previously described for the  $H_{II}$  phase, we have calculated  $d_{pp} = 35.5 \text{ \AA}$ ,  $d_L = 46.5 \text{ \AA}$  and the water diameter of the cylinders  $d_w = 21.7 \text{ \AA}$  which appears to be convenient to accommodate a double-stranded DNA molecule. The smaller value of  $d_w$  in the  $H_{II}^c$  phase of this DOPE/DOPE:PEG(350)-DNA-Mn<sup>2+</sup> complex compared to the that found in the DOPE-DNA-Fe<sup>2+</sup> complex [4], i.e.,  $d_w \cong 25 \text{ \AA}$ , is due to the presence in the phospholipid mixture of PEG-lipid and depends on the packing constraints imposed by the hydrophilic moieties of the PEG-lipid conjugates.

We have observed a similar behaviour in the case of DOPE/DOPE:PEG(350)-DNA-M<sup>2+</sup> mixtures with different metal cations, namely  $M^{2+} = \text{Mg}^{2+}$ ,  $\text{Ca}^{2+}$  (Figs. 5(A) and (B)). In these cases, however, due to the slight differences in the lattice spacing of the two hexagonal structures, the two sets of peaks corresponding to  $H_{II}$  and  $H_{II}^c$  are not as much resolved as in the case of DOPE/DOPE:PEG(350)-DNA-Mn<sup>2+</sup> mixtures. This is evident in Figures 5 (A) and (B) where the arrows indicate the positions of the unresolved peaks corresponding to the  $H_{II}^c$  phase.

In conclusion, this work demonstrates the formation of the triple complex of DOPE/DOPE:PEG(350)-DNA-M<sup>2+</sup> into an inverse hexagonal phase  $H_{II}^c$  when aqueous dispersions of DOPE/DOPE:PEG(350) and metal cations condense with DNA in a self-assembly process. From the point of view of gene therapy applications this finding could be of help to design new structures characterized by good transfection properties. A question still left open by this work, which represents a strong stimulus for further developments of the research in these materials, is the evolution of structure and phase behaviour of the triple complex as the concentration of the pegylated component in the lipid is increased. In fact, based on the results here found for the DOPE/DOPE:PEG(350) aqueous mixtures, the condensation of DNA into structurally more complex structures such as the inverted cubic phase might take place, which should represent an exciting result from both the fundamental and the applicative point of view, in particular in the field of pharmaceutical drug delivery and controlled drug release.

## REFERENCES

- [1] Zhang, S., Xu, Y., Wang, B., Qiao, W., Liu, D., & Li, Z. (2004). *J. Contr. Release*, 100, 165.
- [2] Francescangeli, O., Stanic, V., Gobbi, L., Bruni, P., Iacussi, M., Tosi, G., & Bernstorff, S. (2003). *Phys. Rev. E*, 67, 11904/1.

- [3] Francescangeli, O., Stanic, V., Lucchetta, D. E., Bruni, P., Iacussi, M., & Cingolani, F. (2003). *Mol. Cryst. Liq. Cryst.*, 398, 259.
- [4] Francescangeli, O., Pisani, M., Stanic, V., Bruni, P., & Weiss, T. M. (2004). *Europhysics Lett.*, 67(4), 669.
- [5] Klibanov, A. L., Maruyama, K., Torchilin, V. P., & Huang, L. (1990). *FEBS Lett.*, 268, 235.
- [6] Lasic, D. D. & Papahadjopoulos, D. (1995). *Science*, 267, 1275.
- [7] Uster, P. S., Allen, T. M., Daniel, B. E., Mendez, C. J., Newman, M. S., & Zhu, G. Z. (1996). *FEBS Lett.*, 386, 243.
- [8] Mayhew, E. G., Lasic, D., Babbar, S., & Martin, F. J. (1992). *Int. J. Cancer*, 51, 302.
- [9] Williams, S. S., Alosco, T. R., Mayhew, E., Lasic, D. D., Martin, F. J., & Bankert, R. B. (1993). *Cancer Res.*, 53, 3964.
- [10] Vaage, J., Donovan, D., Mayhew, E., Uster, P., & Woodle, M. (1993). *Int. J. Cancer*, 54, 959.
- [11] Koltover, I., Salditt, T., Radler, J. O., & Safinya, C. R. (1998). *Science*, 281, 78.
- [12] Kenworthy, A. K., Simon, S. A., & McIntosh, T. J. (1995). *Biophysical J.*, 68, 1903.
- [13] Harper, P. E., Rau, D. C., & Parsegian, W. A. (1989). *Macromolecules*, 22, 1780.
- [14] Turner, D. C. & Gruner, S. M. (1992). *Biochemistry*, 31, 1340.
- [15] (1969). *International Tables for X-ray Crystallography*, Vol. I. The Kynoch Press: Birmingham, 71.
- [16] Pisani, M., Fino, V., Bruni, P., Di Cola, E., & Francescangeli, O. (2008). *J. Phys. Chem. B (Letter)*, 112(17), 5276–5278.